OXFORD

Cerebral Cortex, 2023, **33**, 7076–7087
https://doi.org/10.1093/cercor/bhad022
Advance access publication date 23 February 2023
Original Article

Development of brain state dynamics involved in working memory

Ying He[1,†], Xinyuan Liang[1,†], Menglu Chen[1], Ting Tian[1], Yimeng Zeng[1], Jin Liu[1], Lei Hao[1], Jiahua Xu[1], Rui Chen[1], Yanpei Wang[1], Jia-Hong Gao[2,3], Shuping Tan[4], Jalil Taghia[5,*], Yong He[1,6], Sha Tao[1], Qi Dong[1], Shaozheng Qin[1,6,*]

[1]State Key Laboratory of Cognitive Neuroscience and Learning & IDG/McGovern Institute for Brain Research, Department of Psychology, Beijing Normal University, Beijing 100875, China,
[2]Center for MRI Research, Academy for Advanced Interdisciplinary Studies, Peking University, Beijing 100871, China,
[3]McGovern Institute for Brain Research, Peking University, Beijing 100871, China,
[4]Beijing HuiLongGuan Hospital, Peking University, Beijing 100096, China,
[5]Department of Psychiatry & Behavioral Sciences, Stanford University School of Medicine, Stanford, CA 94305, United States,
[6]Chinese Institute for Brain Research, Beijing 102206, China

*Corresponding author: Email: szqin@bnu.edu.cn or taghia.jalil@gmail.com

†Ying He and Xinyuan Liang contributed equally to this work.

Human functional brain networks are dynamically organized to enable cognitive and behavioral flexibility to meet ever-changing environmental demands. Frontal-parietal network (FPN) and default mode network (DMN) are recognized to play an essential role in executive functions such as working memory. However, little is known about the developmental differences in the brain-state dynamics of these two networks involved in working memory from childhood to adulthood. Here, we implemented Bayesian switching dynamical systems approach to identify brain states of the FPN and DMN during working memory in 69 school-age children and 51 adults. We identified five brain states with rapid transitions, which are characterized by dynamic configurations among FPN and DMN nodes with active and inactive engagement in different task demands. Compared with adults, children exhibited less frequent brain states with the highest activity in FPN nodes dominant to high demand, and its occupancy rate increased with age. Children preferred to attain inactive brain states with low activity in both FPN and DMN nodes. Moreover, children exhibited lower transition probability from low-to-high demand states and such a transition was positively correlated with working memory performance. Notably, higher transition probability from low-to-high demand states was associated with a stronger structural connectivity across FPN and DMN, but with weaker structure–function coupling of these two networks. These findings extend our understanding of how FPN and DMN nodes are dynamically organized into a set of transient brain states to support moment-to-moment information updating during working memory and suggest immature organization of these functional brain networks in childhood, which is constrained by the structural connectivity.

Key words: brain states; working memory; development; structural connectivity.

Introduction

Human brain is an open complex system that is dynamically organized to support cognitive and behavioral flexibility as well as rapid adaptation to ever-changing environmental or task demands (Cocchi et al. 2013; Shine et al. 2019). A wealth of recent neuroimaging studies in adults has demonstrated that dynamical organization of functional brain networks is essential to support the performance of various cognitive and affective functions (Braun et al. 2015; Shine et al. 2016; Pedersen et al. 2018; Reddy et al. 2018; Taghia et al. 2018; Gu et al. 2021). Alterations in the dynamical organization of large-scale functional brain networks are linked to cognitive impairments in a variety of psychiatric and neurodevelopmental disorders (Bolton et al. 2020; Cai et al. 2021). As childhood is a critical period, during which the human brain function and structure undergoes protracted development with prominent changes in higher-order cognitive functions such as working memory (Casey et al. 2000), it is pivotal to understand how the dynamical organization of functional brain networks contributes to children's cognitive development. Yet, how large-scale functional brain networks are dynamically organized to support moment-to-moment executive task demands and its link to structural connectivity during childhood remains elusive.

Working memory relies on active engagement and disengagement of multiple brain systems, especially the fronto-parietal network (FPN), that is highly active during task performance (Dosenbach et al. 2006, 2007), and the default mode network (DMN), which is active at rest but suspended during most external tasks (Raichle et al. 2001; Bluhm et al. 2011; Anticevic et al. 2012). One recent study found higher intraconnectivity in FPN with age increasing which mediated the relationship between age and executive performance (Wang et al. 2019). Other recent studies suggest that the segregation and integration of FPN and DMN nodes play an important role in executive function based on the static functional connectivity analysis, which reflects the time-averaged functional brain organization over several minutes (Liegeois et al. 2019; Chen et al. 2022). Examining such functional connectivity in children is the first step in investigating how functional organization of large-scale brain networks develop to support the maturation of cognitive functions. This line of research, however, offers insufficient insights into how these networks features are dynamically organized to support the transient and moment-to-moment changes in information processing during different task demands (Rashid et al. 2016;

Received: February 23, 2022. **Revised:** January 2, 2023. **Accepted:** January 3, 2023

Jin et al. 2017; Bolton et al. 2020). Thus, novel approaches from a dynamical perspective are required to investigate how the FPN and DMN are dynamically organized to support working memory processing and how these dynamical features of brain network organization develop as the brain matures from childhood to adulthood.

There is a growth of research interest to track the dynamical organization of large-scale functional brain networks with the progress of analytic tools in recent years (Hutchison et al. 2013; Sizemore and Bassett 2018). For instance, many studies used sliding-window or related approaches to find increased variabilities of connections with age on whole-brain level or specific functional brain networks (like cognitive control network and DMN) among cognitive tasks (Hutchison and Morton 2015, 2016; Marusak et al. 2017). However, sliding-window approaches are suboptimal to capture transient changes in moment-to-moment task demands due to methodological constraints, including uncertainty, for determining the window length and gaps between windows which can circumvent a reliable estimation of transient neural dynamics (Braun et al. 2015; Marusak et al. 2017; Pedersen et al. 2018). A newly developed unsupervised learning approach, based on Bayesian Switching Dynamic System (BSDS), can mitigate these limitations. This approach identifies the dynamical organization of large-scale functional brain networks as a series of short-lived brain states present at each timepoint with distinct activation and connectivity patterns among brain regions or nodes (Taghia et al. 2018).

Occupancy rate and transition probability are the major dynamical features of these brain states, which reflects the dynamical organization of pivotal brain regions with time (Bolton et al. 2020). For instance, one recent study found that the occupancy rate of certain brain states, characterized by high positive activity in the cingulo-opercular networks and high negative activity in the DMN during resting state, was positively correlated to the subsequent performance of executive functions among children and adolescents (Medaglia, Satterthwaite, et al. 2018). The transition probability of different brain states is referred to the probability switching from one state at a given timepoint to the other states at a next timepoint, suggesting some transitions are more likely than others (Ito et al. 2007; Bassett et al. 2015; Vidaurre et al. 2017; Kringelbach and Deco 2020; Ramirez-Mahaluf et al. 2020). Ryali and colleagues found immature dynamic interactions between DMN, FPN, and salience network, characterized by reduced transition probability among their brain states during the resting state in children (Ryali et al. 2016). Failure to occupy with or transit from specific states not only affects the cognition and behavior, but it is also associated with psychiatric disorders (Damaraju et al. 2014; Kottaram et al. 2019). Furthermore, one recent study on adults using BSDS demonstrated that engaging the optimal state in a timely manner was associated with better behavioral performance and uncovered a hidden transition state which plays a role in reconfiguring task-set during working memory (Taghia et al. 2018). However, no studies, to date, have investigated how dynamic states of the FPN and DMN mature to support working memory processing from childhood to adulthood, and even less is known about how these dynamical maturational changes contribute to working memory performance.

The white matter connectome derived from diffusion tensor imaging has been proved to support the dynamical organization of functional brain networks (Tang et al. 2017). Several previous studies have demonstrated that when given global structural network topology, the theoretical energy cost for brain regions switching to a state with high activation in FPN decreased with age and the process of transition was modulated by task demands (Cornblath et al. 2020; Cui et al. 2020; Braun et al. 2021). These results suggest that the optimization of global structural connectivity with development supports brain transitions, which further contributes to cognition and behaviour. However, which characteristics of white matter connectivity in the FPN and DMN facilitate brain dynamics that support working memory processing remains elusive. Further, evidence from the structure–function coupling emphasizes a ubiquitous role of structural support for functional communication and specialization of a cortical area (Suárez et al. 2020). For instance, lower coupling in the transmodal association cortex compared with somatosensory cortex is linked to more functional flexibility and dynamics in higher-order regions (Baum et al. 2020). One recent study in adults also found that cognitive flexibility was linked with alignment between brain activation and structural network (Medaglia, Huang et al. 2018). Little, however, is known how the structure–function coupling in higher-order regions, like FPN and DMN, modulates brain state dynamics of these networks involved in working memory processing.

To address the above open questions, we set up a developmental functional magnitude resonance imaging (fMRI) study with advanced analytic approaches and a diffusion magnitude resonance imaging (dMRI) study targeting 69 children (aged 7–12 years) and 51 adults (aged 19–24 years) to investigate developmental differences in the dynamical brain states of FPN and DMN regions during working memory task and white matter structural connectivity. The BSDS was implemented to identify the dynamical properties of brain states for the FPN and DMN, including (i) mean activation patterns of distinct brain sates, (ii) occupancy rates and mean lifetime of each state as well as the dynamic evolution of each state, and (iii) transition probabilities among different states. We then examined occupancy rate and mean lifetime of distinct brain states to classify the dominant state and nondominate state representing different mental properties. According to empirical evidence from previous studies on time-varying brain states, we hypothesized that children would exhibit lower occupancy rates, shorter mean lifetime, and less transition probability of key brain states associated with high working memory task demands when compared to adults. Moreover, dynamical properties of key brain states would be associated with working memory performance. Finally, we showed the association between brain dynamics and structural connectivity across FPN and DMN as well as structure–function coupling.

Material and methods

Participants

A total of 120 participants were recruited from the Children School Functions and Brain Development Project (CBD, Beijing Cohort). All participants with mean accuracy for 0-back condition >50% and low head motion (max displacement <1 mm) were selected for later analysis, including 69 children from the age range between 7 and 12 years old (mean = 9.43 ± 1.54) and 51 healthy adults from the age range between 19 and 24 years old (mean = 21.76 ± 1.64). Written informed consent was obtained from every participant. For children, written informed consent was obtained from 1 of their parents or legal guardians. All of the participants reported no history of vision problems, no history of neurological, or psychiatric disorders, and no current use of any medication or recreational drugs. Demographics of 69 children and 51 adults are listed in Supplementary Table S1.

For diffusion magnetic resonance imaging (dMRI) data, we excluded 1 participant due to the missing dMRI scan, 2 participants due to excessive head motion (maximum head

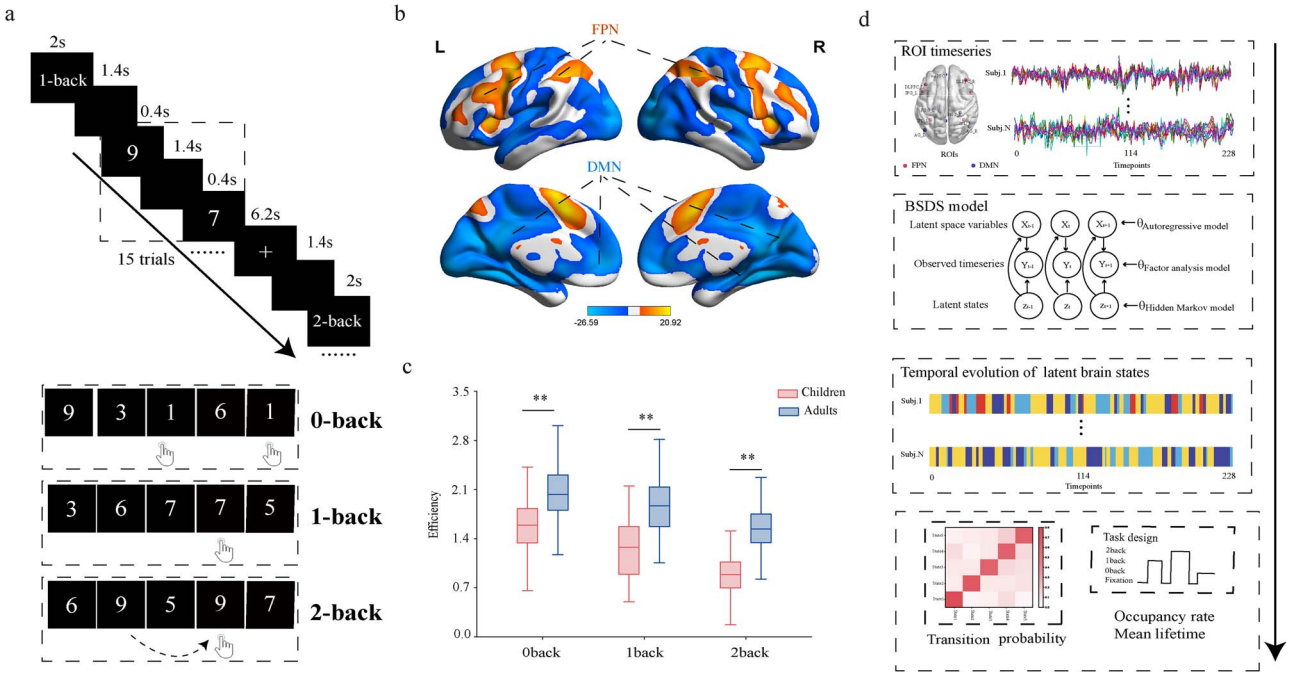

Fig. 1. WM task effect and an overview of analysis process. a) Experimental paradigm of numerical 0-, 1-, and 2-back working memory task conditions. b) Brain regions activated and deactivated during 2-back condition in all subjects. c) Efficiency of children and adult group as a function of task loads (0-, 1-, and 2-back). Efficiency: accuracy divided by reaction time (independent-sample *t* test, $^{**}P < 0.01$). d) Schematic illustration of BSDS analysis. At first, we defined 12 ROIs of FPN and DMN and extracted ROIs time series of each subject. And then, BSDS model was applied to the preprocessed time series. Finally, we got the temporal evolution of states from BSDS model and extracted the dynamic properties of states: occupancy rate, mean lifetime, and transition probabilities of states.

motion >3 mm), and 1 participant due to serious signal dropout. After these, dMRI images from 65 children (mean = 9.48 ± 1.53) and 51 adults were included in our dMRI analysis.

Experimental design

Participants were asked to complete a blocked-design numerical *n*-back task consisting of 3 conditions (0-back, 1-back, and 2-back) during scanning (Xiong et al. 2021). Within each block, a random digit sequence consisting of 15 digits was presented one by one (Fig. 1a). In the 0-back condition, participants were required to press the button when the number currently displayed on the screen was "1." In the 1-back condition, participants were required to press the button when the number currently displayed was the same as last one. In the 2-back condition, participants were required to press the button when the number currently displayed was same as the previous 2. Every digit was presented 400 ms followed by a 1,400-ms empty screen. The task consisted of 12 blocks with randomly assigned 4 blocks for each condition. Before scanning, participants were adequately trained to ensure the instruction was fully understood. Stimuli were presented via E-Prime 2.0 that was widely used in psychological experiments (http://www.pstnet.com; Psychology Software Tools, Inc). Task performance was measured by both accuracy (defined as the percentage of correct answers) and reaction time (defined as the length of time from stimulus onset to button press) for each condition separately. We also calculated the efficiency (ACC/RT) as a measure of behavioral performance.

Functional imaging data acquisition and preprocessing

Imaging data were acquired from Siemens 3.0 T scanner (Magnetom Prisma syngo MR D13D, Erlangen, Germany) using a 64-channel head coil with a T2*-sensitive echo-planar imaging (EPI) sequence based on the blood oxygenation level-dependent (BOLD) contrast. Thirty-three axial slices (3.5 mm thickness and 0.7 mm skip) parallel to the anterior and posterior commissure line and covering the whole brain were imaged with the following parameters: repetition time (TR) = 2,000 ms, echo time (TE) = 30 ms, flip angle = 90°, voxel size = 3.5 × 3.5 × 3.5 mm^3, field of view (FOV) = 224 × 224 mm^2. The *n*-back task consisted of 232 volumes. Before the acquisition of functional images, each participant's high-resolution anatomical images were acquired through 3D sagittal T1-weighted magnetization-prepared rapid gradient echo with a total of 192 slices: TR = 2,530 ms, TE = 2.98 ms, flip angle = 7°, inversion time = 1,100 ms, voxel size = 0.5 × 0.5 × 1.0 mm^3, acquisition matrix = 256 × 224, FOV = 256 × 224 mm^2, BW = 240 Hz/Px, slice thickness = 1 mm.

Brain images were preprocessed using statistical parametric mapping (SPM12, https://www.fil.ion.ucl.ac.uk/spm/software/spm12/) (Friston, HBM-1994) based on MATLAB platform. The first 4 volumes of functional images were discarded for signal equilibrium and participants' adaptation to scanning noise. Remaining images were preprocessed following a standard routine: corrected for slice acquisition time and realigned for head motion correction, coregistered to each participant's gray matter image segmented from the corresponding high-resolution T1-weighted image, spatially normalized into a common stereotactic Montreal Neurological Institute (MNI) space and resampled into 2 mm isotropic voxels, and spatially smoothed with a 6-mm full-width half-maximum Gaussian kernel.

Univariate general linear model analysis

To assess the task-related neural response in the *n*-back task, the 0-back,1 back, and 2-back conditions were modeled as 3 separate boxcar regressors and convolved with the canonical hemodynamic response function built in SPM12. In addition,

6 head motion parameters from the realignment procedure were included to regress out the variability elicited by the head movement. We used high-pass filtering using a cutoff of 1/128 Hz and corrections for serial correlations in fMRI using a first-order autoregressive (AR) model in the general linear model (GLM) framework. Relevant contrast parameter estimate images were initially generated at the individual-subject level, including 3 regressors (0-back, 1-back, and 2-back), 1-back versus 0-back, 2-back versus 0-back, and 2-back versus 1-back.

One-way ANOVA was applied to investigate the activation pattern of 0-back, 1-back, and 2-back for all participants (regardless of adults and children) in the second-level analysis. Significant clusters were determined using a threshold of $P < 0.001$ with family-wise error corrections for multiple comparisons based on nonstationary suprathreshold cluster-size distributions, which were computed using Monte Carlo simulations(Swendsen and Wang 1987). The contrast of interest was WM load effect: 2-back.

Regions of interest definition

The ROIs in the FPN and DMN were derived from the Neurosynth platform, a large-scale and automated synthesis of fMRI data (http://neurosynth.org), by using "working memory" and "default mode network" as search terms, respectively. These ROI masks were then refined by using a height threshold of z-score > 3.0 and a spatial extent cluster size of >30 voxels, which was similar to previous studies (Zhuang et al. 2022). We extracted the positive activation map from 2-back contrast and overlapped this map with the mask using "working memory" as a search term (Supplementary Fig. 1). The same way was applied to the negative activation map for "default mode network" mask. This procedure produced 6 ROIs within the FPN, including the bilateral dorsal lateral prefrontal cortex (DLPFC_L and DLPFC_R), the bilateral inferior frontal gyrus (IFG_L and IFG_R), and the bilateral inferior parietal lobule (IPL_L and IPL_R), and 6 ROIs in the DMN, including the ventral medial prefrontal cortex, the posterior cingulate cortex, the bilateral angular gyrus (AG_L, AG_R), and the bilateral parahippocampal gyrus (PHG_L, PHG_R) (Supplementary Table S2). Regional mean BOLD time series were extracted from each mask and were further linearly detrended. After demeaning time series, signals of white matter, and cerebrospinal fluid, 6 motion parameters were extracted and regressed them out from the resulting data.

BSDS model

The BSDS model assumes that the ROI time series can be described as a finite number of states repeating or switching with time, each of which is represented by a multivariate Gaussian distribution that is parameterized by a mean vector and a covariance matrix. This method applies hidden Markov model (HMM) to latent space variables of observed data, which differs from previous studies that apply HMM directly to observed electro-physiological and fMRI data (Vidaurre et al. 2016, 2017, 2018). The following is a brief description about interference and derivations of the generative model. Observed fMRI data are modeled by a probabilistic factor analysis model, including a series of latent space variables generated from an AR process. A first-order Markov chain through an HMM is applied to these latent space variables. Posterior distributions of all model parameters are inferred by Bayesian inference using Bayes' theorem to combine priors with data. Considering a parametric Bayesian formulation of BSDS, variational inference is used for learning about the model parameters and inference of the latent variables.

The normalized BOLD time courses for each ROI were temporally concatenated across all subjects, including adults and children. We integrated 2 groups to run the BSDS model because this method could benefit for model fitting, which is constrained by BSDS itself and did not require matching brain states between separate models. The BSDS model was applied to the time courses which could provide the temporal evolution of the states, the occupancy rate and mean lifetime of states, the transition probability matrix, and mean and covariance of states. Occupancy rate is defined as the proportion of time spent in a state, whereas mean lifetime is the average time that a state persists per each visit. Transition probability characterizes the probability of any state switch to another. We repeated BSDS process about 10 times and chose the best model for further analysis, where the best model corresponds to the one that achieves the highest lower bound on the marginal likelihood of data.

Diffusion-weighted image acquisition and data preprocessing

All diffusion-weighted images were acquired on a 3T Siemens Prisma scanner with a 64-channel head coil. The parameters as follows: TR = 7,500 ms, TE = 64 ms, acquisition matrix = 112×112, FOV = 224×224 mm^2, slices = 70, slice thickness = 2 mm, BW = 2,030 Hz/Px, 64 diffusion weighted directions with $b = 1{,}000$ s/mm^2, and 10 images without diffusion weighting ($b = 0$ s/mm^2).

The dMRI data were preprocessed following denoising (Tournier et al. 2019), removing Gibbs ring (Kellner et al. 2016), eddy current artifacts correction (Andersson and Sotiropoulos 2016), signal dropout correction (Andersson et al. 2016, 2017), EPI susceptibility distortions correction, and bias correction (Tustison et al. 2010). Details about the diffusion-weighted images acquisition parameters and data preprocessing analysis are available in Liang et al. (2022). For each voxel, we estimated the diffusion tensor (Basser et al. 1994) and calculated the fractional anisotropy (FA) (Westin 1997) using MRtrix3.

White matter tractography

To reconstruct the white matter tracts, we performed the generalized q-sampling imaging algorithm-based deterministic fiber tracking (Yeh et al. 2010) in each individual native dMRI space using DSI Studio software (https://www. Nitrc.org/projects/dsistudio). Specifically, we first retained the voxels with FA values > 0.1 to form the seed mask. The tractography was terminated if it reached a voxel with an FA < 0.1 or it's turning angle being > 45°. For each subject, 10 million streamlines were generated. Streamlines < 6 mm or > 250 mm were discarded. Next, each subject's T1 image was coregistered to the mean b0 image and the transformed T1 image was then nonlinearly transformed to the ICBM152 T1 template in the MNI space. We invert the transformations and applied them to warp the 12 ROIs derived from functional brain from the MNI space, which were dilated by 1 voxel to the dMRI native space (Shu et al. 2011). For each pair of ROIs, they were considered anatomically connected if there were at least 1 streamline with 2 endpoints located in these 2 regions (Zalesky et al. 2010). Finally, for each subject, we calculated the mean FA values across all voxels in the tract between each 2 ROIs to the weighted white matter connectivity matrix.

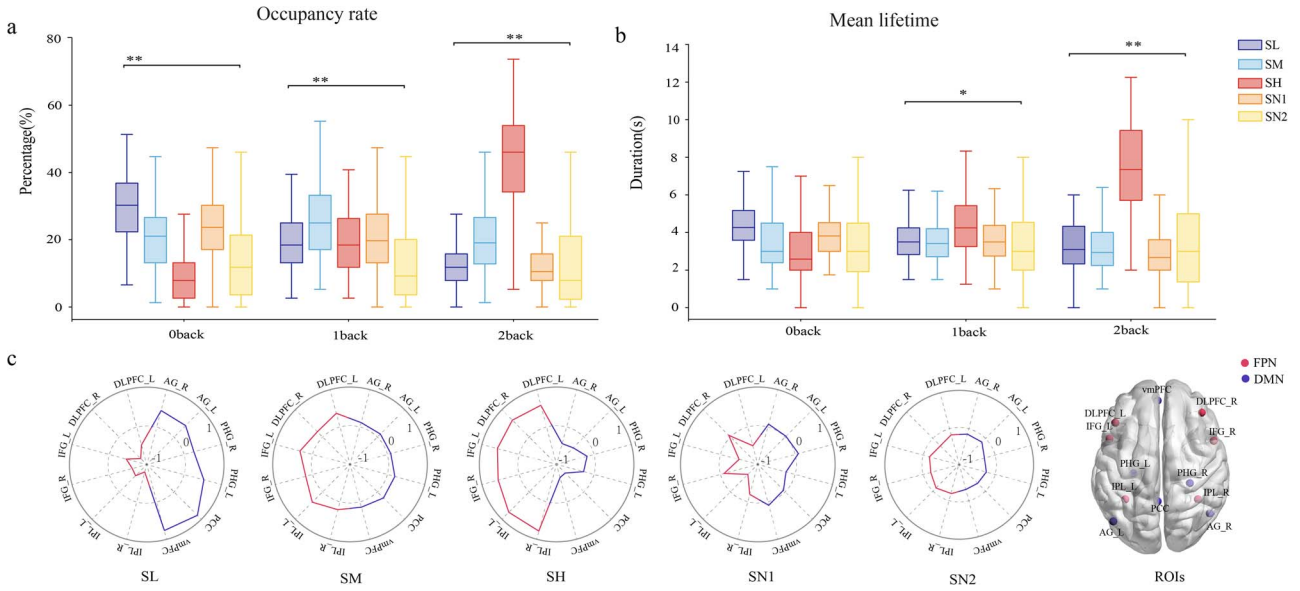

Fig. 2. Brain-state properties and their mean activation distribution during working memory. a) Occupancy rates of brain states for the 3 states which dominate the 0-back, 1-back, and 2-back task conditions named as SL, moderate-demand state (SM) and SH. The remaining states are SN1 and SN2. The star symbol denotes that the occupancy rate of this state are significantly higher than all the other states (paired *t* test FDR-corrected, *: all *P* values < 0.05, **: all *P* values < 0.01). b) Mean lifetime of brain states for SH which dominates 1-back and 2-back task blocks. c) Mean activation pattern of brain states. SH is marked as the highest frontoparietal activity and the SL shows the lowest. For SM, FPN is slightly higher than 0 and DMN is close to 0. SN1 and SN2 both show lower activity of 2 networks. ROIs are determined using a combination of activation map from GLM and templates from Neurosynth. We draw spheres to illustrate the coordinates of these nodes for better presentation, but actually clusters of ROIs were used for extracting the time series.

Measure structure-function coupling in brain networks

First, functional connectivity between each pair of FPN and DMN was estimated as the Pearson correlation coefficients between the mean time series mentioned above. So, for each participant, a 12×12 weighted matrix encoding the functional connectome was constructed. Connectivity profile was extracted from the functional and structural connectivity matrixes and was represented as vectors, including all edges for each participant. And then, the structure–function coupling was measured as the Spearman rank correlation between non-0 element of structural and functional connectivity profiles (Baum et al. 2020). Finally, the rank correlation was Fisher z-transformed for later analysis.

Results

Latent brain states of FPN and DMN regions involved in working memory

Behaviorally, children exhibited lower efficiency in each condition as compared to adults (Fig. 1c). We then investigated the dynamic functional organization of large-scale brain networks during WM processing, with a focus on the distributed regions of the FPN and DMN. The BSDS identified a total of 5 brain states. The distribution of the occupancy rate and mean lifetime of brain states in each condition is mostly similar across the two groups (Supplementary Fig. 2), so we did the next analysis about dominant states based on all groups. Separate paired *t* tests were then conducted to examine whether there were dominant brain states for 3 WM loadings. As shown in Fig. 2a, these analyses revealed 3 dominant states for 0-back, 1-back, and 2-back conditions, as their occupancy rates were significantly higher than any other states (all $t_{(119)} \geq 3.42$, *P* values < 0.001 FDR-corrected, all Cohen's $d \geq 0.50$). Similar to one previous study (Taghia et al. 2018), we referred these 3 dominant states to a low-demand state (SL), moderate-demand state (SM), and high-demand state (SH), respectively. The remaining states were designated as nondominated states 1 and 2 (SN1 and SN2). Parallel analyses revealed significantly higher mean lifetime of SH than the other states in 1-back and 2-back conditions (all $t_{(119)} \geq 2.963$, all *P* values < 0.01 FDR-corrected, all Cohen's $d \geq 0.39$, Fig. 2b).

Each state had distinct patterns of mean activation and connectivity patterns among 6 nodes within FPN and 6 nodes within DMN (as shown in Fig. 2c and Supplementary Fig. 3). Since the time series input to the BSDS were normalized with zero mean and unit standard deviation, the zero is equal to the mean level of brain activity during the whole task (Kottaram et al. 2019). The negative activation (below average) means a relatively low level of BOLD activity and positive activation (above average) means a relatively high level of BOLD activity. SH showed the highest activity in nodes of the FPN and the lowest in nodes of the DMN, while SL had a completely opposite pattern with lowest activity in nodes of the FPN and highest activity in DMN nodes. SM was a state with slightly higher activity than 0 in the FPN nodes and close to 0 for DMN nodes. The remaining 2 states both showed low-level activity (almost <0) in 2 networks, especially the mean activity of all nodes for SN2 were less than 0. These results indicate that three cognitive-demand conditions could be characterized by one dominant brain state each interspersed with other non-dominant states.

Developmental differences in WM-related brain states of FPN and DMN

Next, we investigated developmental differences in the properties of dynamic brain states associated with WM between children and adults. Separate independent sample *t* tests were conducted to investigate the differences in the occupancy rate and mean lifetime of SH from childhood to adulthood (Fig. 3).

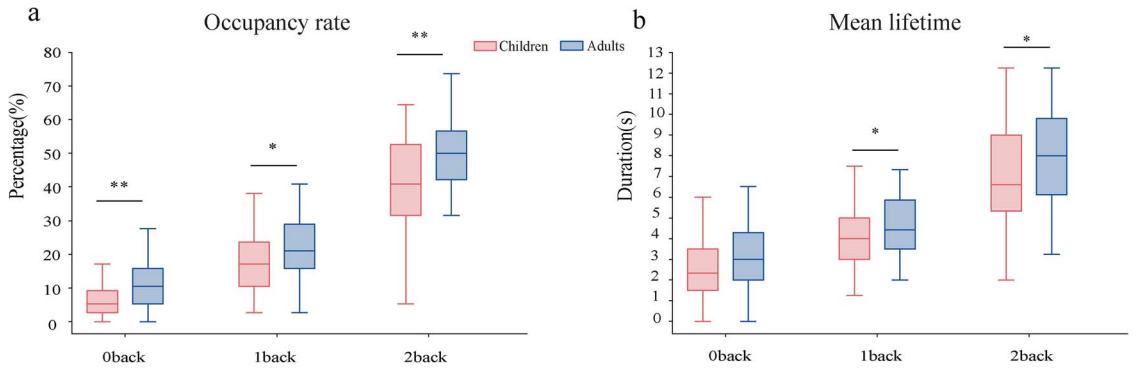

Fig. 3. Occupancy rate and mean lifetime of key brain state differ between children and adults. a) Comparison of occupancy rate for SH during different conditions between 2 groups. Adults have a higher occupancy rate of SH than children in every condition (independent-sample t test, *: $P < 0.05$, **: $P < 0.01$). b) Comparison of mean lifetime for SH during different conditions between 2 groups. Adults have a higher mean lifetime of SH than children in 1-back and 2-back conditions (independent-sample t test, *: $P < 0.05$).

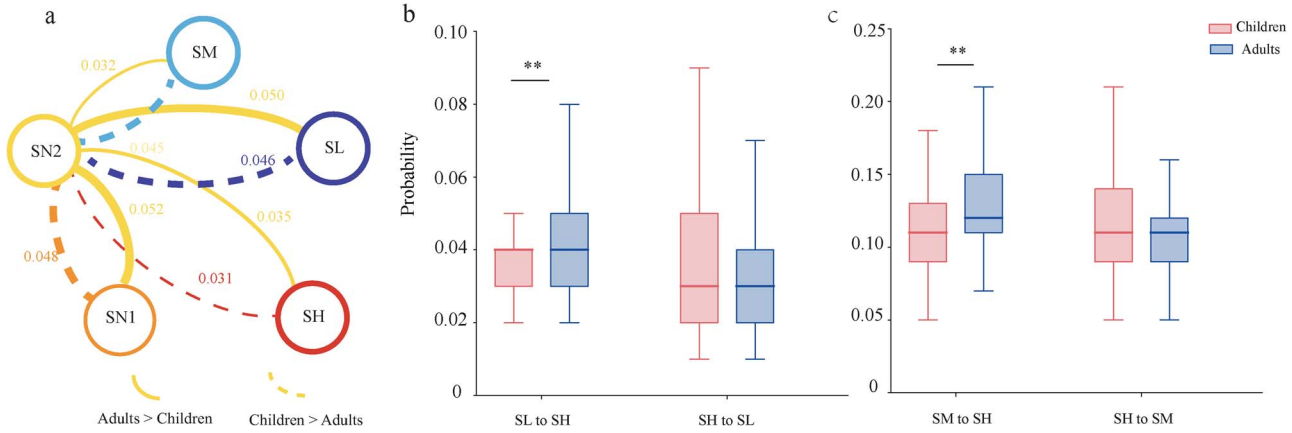

Fig. 4. Developmental difference of dynamic transition properties of brain states. a) Illustration of top 40% significant between-group differences of transition probabilities. Solid lines represent that the transition probability of children is significantly higher than adults. Dotted lines represent the opposite. (b and c) Comparison of transition probability about dominant states reveals that adults have higher probability from SL and SM to SH compared with children, but there is no difference of transition probability from SH to SM and SL (independent-sample t test, **: $P < 0.01$).

Compared to children, adults had a higher occupancy rate of SH in all 3 task conditions (0-back: $t_{(118)} = -3.760$, $P < 0.001$, Cohen's $d = -0.72$; 1-back: $t_{(118)} = -1.997$, $P = 0.048$, Cohen's $d = -0.37$; 2-back condition: $t_{(118)} = -3.894$, $P < 0.001$, Cohen's $d = -0.70$). During 1-back and 2-back conditions, adults had a higher mean lifetime of SH than children (1-back: $t_{(118)} = -2.156$, $P = 0.049$, Cohen's $d = -0.38$; 2-back: $t_{(118)} = -2.451$, $P = 0.017$, Cohen's $d = -0.45$). Conversely, children had a higher occupancy rate and mean lifetime of SN2 with relatively uniform activity in FPN and DMN in each condition (Supplementary Fig. 4). These results indicate that, compared with adults, children had a lower fractional occupancy rate and mean lifetime of brain state with the highest FPN activity and lowest DMN activity that dominant to highest task demand condition.

Developmental differences in temporal transitions among WM-related brain states

Transition probabilities of each subject were derived from the BSDS model. We first averaged all the probabilities within groups (Supplementary Fig. 5a and b). To further examine the developmental differences in dynamic properties—transition probability among different brain states during WM task between children and adults, separate independent 2-sample t tests after FDR correction revealed all differences in the transition probabilities of each pair of brain states Supplementary Fig. 5c. Based on the results, we then examined their maximum differentiation between two groups. An illustration about the top 40% (both absolute values of mean differences and effect size of t test) significant between-group differences of transition probabilities (except self-transitions) after multiple comparisons is shown in Fig. 4a. The dotted line means children had higher value than adults and the solid line means the opposite. Colors of lines represent which state switches to other states. Children had higher probabilities transiting to a state of SN2 which was characterized by lower activity than that of both FPN and DMN from other states (all $t_{(118)} \geq 5.858$, all P values < 0.001 FDR-corrected, all Cohen's $d \geq 1.055$). But adults showed higher transition probabilities from SN2 to other states (all $t_{(118)} \leq -4.163$, all P values < 0.001 FDR-corrected, all Cohen's $d \leq 0.761$). These results indicate that children were more prone to an inactive state during WM task as compared with adults.

We further investigated developmental differences in the transition probabilities among dynamic brain states dominant to each of the 3 WM loads. Separate, independent 2-sample t tests mentioned above revealed that adults showed higher transition probabilities of SM and SL to SH than children (SM to SH: $t_{(118)} = -4.005$, $P < 0.001$, Cohen's $d = -0.73$; SL to SH: $t_{(118)} = -3.311$, $P = 0.002$, Cohen's $d = -0.63$; FDR corrected for multiple comparisons, Fig. 4b and c). However, for the transition from SH to SL and SM, there was no significant difference between the two groups (SH to SM: $t_{(118)} = 1.092$, $P = 0.33$, Cohen's $d = 0.20$; SH to SL: $t_{(118)} = 0.024$, $P = 0.98$, Cohen's $d = 0.004$; FDR corrected

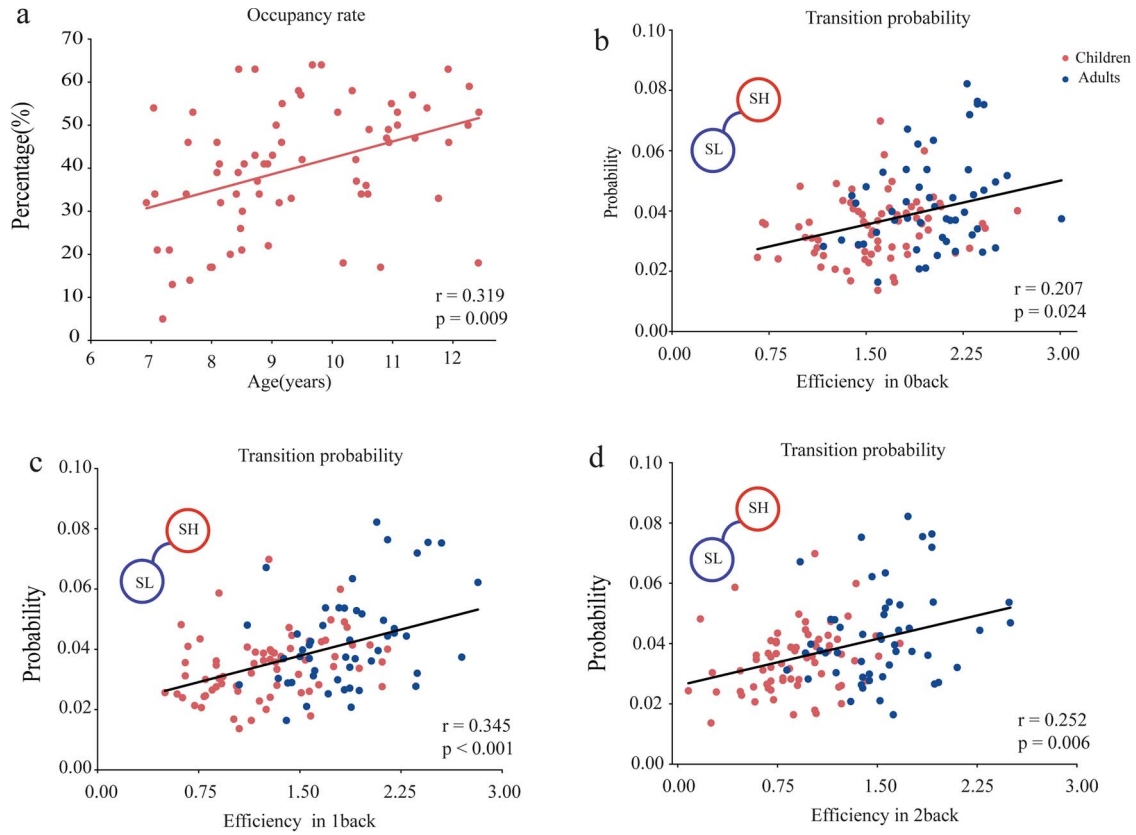

Fig. 5. Brain-state dynamics associated with age and behavioral performance. a) There is a significant positive correlation between occupancy rate of SH in 2-back condition and age within children group. b–d) Transition probability of SL to SH is positively correlated with behavioral performance in 0-back, 1-back, and 2-back conditions, respectively (0-back: $r = 0.207$, $P = 0.025$; 1-back: $r = 0.345$, $P < 0.001$; 2-back: $r = 0.252$, $P = 0.009$; FDR corrected for multiple comparisons).

for multiple comparisons, Fig. 4b and c). These results indicate a lower transition probability from a low-load brain state to a high-load brain state in children than adults.

Brain-state dynamics linked to working memory performance and age-related increases

We further examined age-related changes in the properties of dynamic brain states during childhood. After controlling the gender, head motion, and behavioral performance, we found a significantly positive correlation between age and occupancy rate of SH (r = 0.319, P = 0.009, Fig. 5a). A marginally significant positive correlation was found between the mean lifetime of this state and age (r = 0.237, P = 0.056) (Supplementary Fig. 6a). These results indicate that the high-load state exhibits an increase as a function of age during childhood. To investigate whether WM-related brain states could predict the WM performance and age, partial correlation analyses were applied to examine the associations between the transition probability of SL switching to SH and behavioral performance of two groups. Gender, head motions, and age were included as covariates of no interest in the partial correlation analyses. We found that the transition probability from SL to SH was positively correlated with the behavioral performance in all of 3 conditions (0-back: $r = 0.207$, $P = 0.024$; 1-back: $r = 0.345$ $P < 0.001$; 2-back: $r = 0.252$, $P = 0.006$; all P values were FDR corrected) (Fig. 5b–d). We also investigated whether the transition probability from SM to SH was correlated with WM performance. This analysis revealed a significantly positive correlation in the 1-back condition (0-back: $r = 0.154$, $P = 0.097$; 1-back: $r = 0.240$, $P = 0.009$; 2-back: $r = 0.036$, $P = 0.669$; all P values were FDR corrected) Supplementary Fig. 6b–d. These results indicate that the higher probability of a high-load state switching to an SL contributes to better performance during the working memory task.

WM-related brain-state dynamics associated with structural connectivity and structure–function coupling

To address the association between brain structure and WM-related state dynamics, we first examined the differences of structural connectivity between children and adults. Independent 2-sample t test was applied to the mean FA between two groups, and it was found that children showed lower mean FA than adults ($t_{(114)} = -4.705$, $P < 0.001$, Cohen's $d = -0.881$, Fig. 6a). We also found a significant correlation between age and mean FA in children after regressing out covariants as gender and head motion ($r = 0.256$, $P = 0.0461$, Fig. 6a). These results indicate that structural connectivity across FPN and DMN increases with age during childhood. Thereafter, we further investigated the relationship between brain dynamics and structural connectivity. Partial correlation analysis found that transition probability from SL to SH positively correlated with mean FA after regressing out age, gender, head motion, and behavioral performance ($r = 0.203$, $P = 0.0319$, Fig. 6b). These results indicate that the increasement of structure connectivity across FPN and DMN could facilitate the brain transitions from low-to-high demand states.

Finally, we investigated the correlation of transition probability from SL to SH with structure–function coupling. Structure–function coupling was estimated by correlation

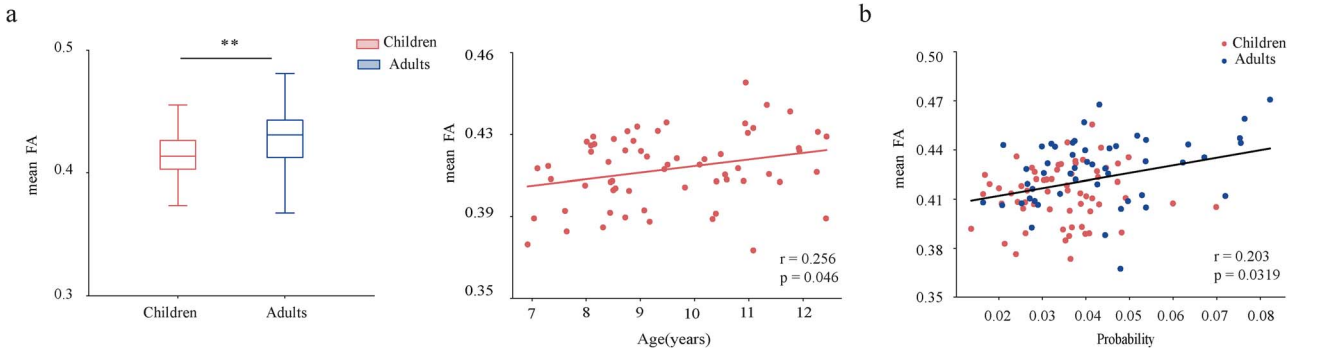

Fig. 6. Structural connectivity increases with development and its link to brain state properties. a) In comparison with adults, children have lower mean FA across FPN and DMN (left). And, mean FA increases with age within children group. b) Transition probability of SL to SH is positively correlated with mean FA across FPN and DMN ($r = 0.203$, $P = 0.0319$).

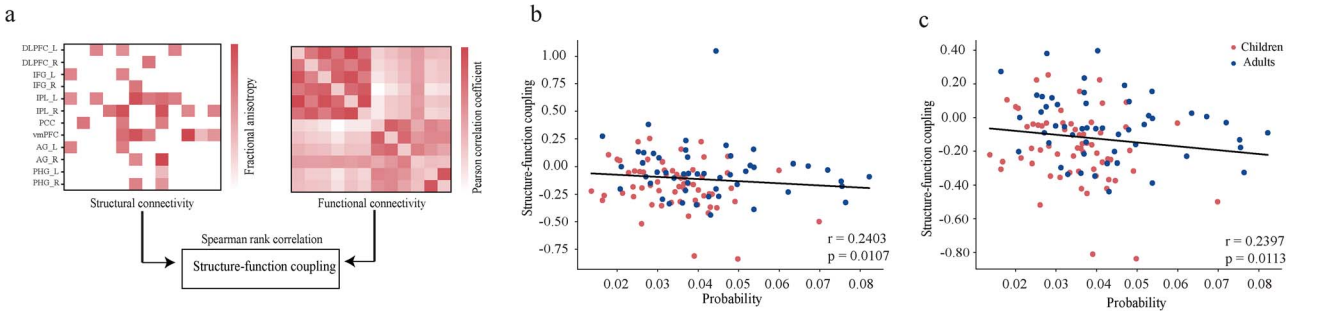

Fig. 7. Structure–function coupling negatively associated with brain stater proporties. a) Illustration of measuring structure–function coupling. For each subject, we computed the structural and functional connectivity matrixes, respectively. Structure–function coupling was then measured as the spearman rank correlation between non-0 elements of structural and functional connectivity matrixes. b) Scatter plot shows negative correlation between structure–function (based on time-averaged functional connectivity matrix) coupling and transition probability from low-to-high demand states without exclusion of outliner ($r = -0.2403$, $P = 0.0107$). c) Same plot as (b) only with exclusion of an outliner ($r = 0.2397$, $P = 0.0113$).

between non-0 elements of structural connectivity matrix and time-averaged functional connectivity matrix. We found both significant negative correlation of structure–function coupling and transition probability before excluding outliner ($r = -0.2403$, $P = 0.0107$) and after excluding outliner ($r = 0.2397$, $P = 0.0113$) when controlling the covariants as described above (Fig. 7). These results indicate weaker structure–function coupling is linked to more brain transitions.

Discussion

By leveraging a novel unsupervised BSDS method, we investigated developmental differences in the brain-state dynamics of FPN and DMN nodes involved in WM processing in children and adults. We identified a brain state with the highest activity in FPN dominant to high WM task demand (namely SH), and this state presented as less frequent but was more short-lived in children and its occupancy rate increased with age. In comparison to adults, children were more likely to switch to inactive states and it was more difficult to attain SH from the SL that was positively correlated with the WM performance. Further, we found a stronger structural connectivity in adults than children, but weaker structure–function coupling indicated higher probability from low-to-high demand states. Our findings suggest immature dynamical organization of FPN and DMN nodes and its link to the structural architecture of these systems involved in WM during childhood.

We observed several aspects of prominent developmental differences in the dynamical properties of brain states involved in WM processing between children and adults. The first aspect is that children exhibited less frequent and shorter duration in SH, especially in the 2-back condition. Interestingly, the SH occupied the most and persisted for the longest duration during the 2-back condition and was accompanied with the highest mean activity in FPN nodes and the lowest activity mean activity in DMN nodes. This pattern of result is analogous to previous conventional GLM activation studies (Curtis and D'Esposito 2003; Leung et al. 2004). For instance, higher recruitment of FPN is closely related to holding more task-required information on-line, making more efforts to monitor and manipulating processes as working memory load increases (Owen et al. 2005; Alvarez and Emory 2006; Ma et al. 2012). These results suggest that children showed a lower engagement along with less maintenance of the state related to high-level cognitive allocation frequently and constantly when compared to adults.

Demand-changing cognitive processes are always affected by unobserved latent factors (e.g. mind wandering, mental fatigue, and motivation) across time (Wascher et al. 2014; Gergelyfi et al. 2015). These latent factors are insufficient to capture by using static or length-average method limited by external task condition in previous conventional studies (Seghier and Price 2018; Bolton et al. 2020). By implementing BSDS, our results found that children had more occupancy rate and longer mean lifetime of a state that had low activity in both FPN and DMN nodes. Analogous state which characterized by relatively consistent low-level activity of brain networks occurred frequently in resting condition (vander Meer et al. 2020). Prior study also suggests that this kind of state might be related to poor behavioral performance and negative symptoms (Kottaram et al. 2019). Based on that, we speculate that children may be affected

more by these latent factors, which represents the dynamical organization mentioned above. Furthermore, the sources of age-related changes in dynamic states could be constrained by anatomically frameworks (Deco et al. 2011; Avena-Koenigsberger et al. 2018; Baum et al. 2020). One previous study found that more segregation between modules and enhanced hub edges supporting flexible communication between functional brain network contributed to both specialization and coordination over development (Baum et al. 2017). Immature brain structure and function in children, however, may lead to the persistence of this activity pattern that is suboptimal to support the performance of flexible task demands. We also found that the occupancy rate of the SH had a significant age effect within children group, suggesting that the dynamical fluctuation of brain statess plays a critical role during the developmental course. Together, our study suggests that dynamical organization of the FPN and DMN nodes cannot engage in and maintain an adult-like level of the SH during demand-changing WM task in children.

By another aspect, our study found distinct transition probability patterns during WM between children and adults. Occurrence rate and mean lifetime mainly reflect the temporal changes in a certain brain state, whereas the transition probabilities between brain states are more about the moment-to-moment changes among these states. The most prominent difference is that children were more likely to switch to the state whose activities of FPN and DMN were consistent and both lower than mean level of brain fluctuation during the whole session. As mentioned above, this state may represent a more inactive pattern closely related with the resting state (vander Meer et al. 2020). This result suggest that children were more likely to shift into a task-irrelevant state regardless of what the last state was. It parallels with one previous behavioral study which found that young children had more difficulty in concentrating on the present task consistently (Akshoomoff 2002).

Besides the prominent differences around the inactive states, we also found that children had less probabilities transiting from SL and SM to the SH like adults, but the transition probabilities from SH to lower demand did not show significant differences. One recent study suggests that accessing 2-back state from 0-back state for healthy adults during working memory requires more control energy than vice versa (Braun et al. 2021). Control energy is theoretically defined as the effort of brain regions to achieve the desired activation pattern based on the interconnecting white matter tracts (Gu et al. 2015), which reflects the transition between distinct brain activation patterns and was modulated by brain structure. This is supported by evidence from behavioral studies, suggesting that switching to a difficult task from the easy task always cost more time than switching in the opposite direction (Rubinstein et al. 2001; Yeung and Monsell 2003). So, opposite transition directions between distinct task demands had different levels of difficulties for subjects according to both neuroimaging and behavioral findings. Previous studies found that switching cost (i.e. larger reaction time) decreased with age in children and showed a greater cost than adults (Reimers and Maylor 2005; Crone et al. 2006; Tomporowski et al. 2008). Recent study found that the functional transitions to an FPN-activated state (seems like SH in our study) requires less energy cost with age increases because of optimization of topological distribution from white matter structure during development. Although these developmental studies did not examine the differences of opposite transition directions between different task demands, they demonstrated that, at least, for children, switching to a more difficult task condition or a more activated brain states cost more time or control energy than adults according to the behavioral and neuroimaging studies. Based on findings from these studies, we speculate that switching to an optimal state-related high cognitive-demanding condition from a state-related low cognitive-demanding condition for children requires more cognitive allocation and more mature structure which differs significantly between children and adults. But the opposite switch did not show the same high requirement, so this represents little differences between children and adults. We also found the behavioral performance linked to transition probabilities from the SL to SH. The significant positive correlation revealed being more prone to aforementioned efficient transition of brain states contributed to better task performance. Further, we found that this transition probability was more related to reaction time in comparison to accuracy. It may suggest that the dynamical transitions of brain states is more beneficial for a faster reaction speed. Our results suggest that children exhibit immature dynamics of brain-state switching between distinct WM demands, which is closely related with behavior.

The divergence of these transient brain states between children and adults is mainly reflected by their distinct dynamical nature, including occupancy rates and transition probabilities. Dynamics of canonical brain networks are proved to capture more task-evoked information and even to perform better in predicting disease (Rashid et al. 2016; Jin et al. 2017; Liegeois et al. 2019). Working memory is a fundemental cognitive ability that is broadly involved in daily life and is closely related to academic performance in children (Iuculano et al. 2011; Dumontheil and Klingberg 2012). Thus, our findings extend this existing knowledge on the dynamical organization of FPN and DMN nodes underlying the working memory in children, which could provide new insights for typical and atypical development and even for the classification on related developmental disorders such as ADHD. Moreover, our study provides age-related charateristics of the moment-to-moment transition probability between WM-related brain states during childhood. Clarifying transitions of these brain states may provide new inspiration for interventions on diseases, which may allow the possibility of forcing an efficient transition using an external stimulation like tDCS and TMS (Deco et al. 2019).

Furthermore, we found that children exhibited a lower structural connectivity strength across FPN and DMN than adults and showed age-related increase in the strength from 7 to 12 years of age during childhood. Our findings are consistent with previous studies. This demonstrates a protracted maturation pattern of white matter maturation during childhood (Lebel et al. 2012; Lebel and Deoni 2018). Moreover, increasement of mean FA is associated with higher transition probability from SL to SH. This result suggests that stronger structural connectivity contributes to effective brain dynamics which support behavior. The increase of FA reflects axonal myelination, which facilitates neuronal communication by enhancing signaling speed (Tomassy et al. 2016; Lebel et al. 2019). Previous studies have suggested that structural connectivity optimized with development better controls the functional transitions of brain states (Tang et al. 2017). Our present finding further emphasizes the optimization characterized by stronger structural connectivity, which suggests a more effective neuronal communication to support better transitions. It has been proven that the coupling of brain function and structure reflects the flexibility of functional communication in brain regions (Baum et al. 2020). We found a weaker coupling between structural connectivity and time-averaged functional connectivity relating with higher transition probability. Lower structure–function coupling that reflects the divergent pattern

between structural network and functional network may support the functional flexibility and dynamical recruitment of brain regions when faced with diverse task demands (Yeo et al. 2015), so suggesting more flexible dynamics. Together, we speculate that our results may suggest that a stronger structural connectivity, but lower coupling with functional connectivity, could contribute to effective brain dynamics.

Several limitations should be considered for our findings. First, the BSDS is a useful computational tool for characterizing the dynamical latent brain states, but these states are the results of a mathematical fitting model of observed data which needs constricted assumption about model parameters. Second, we used a cross-sectional design that lacks the tracking of each individual's developmental profiles in dynamical brain states during WM. Finally, our present study only focused on FPN and DMN nodes rather than the whole brain network due to the complexity of the model and extensive computation resources. Future studies are required to mitigate these limitations.

Conclusion

In conclusion, our study demonstrates an immature dynamical organization of the FPN and DMN nodes during WM, which is characterized by less occupancy rate of high-demand brain state and more transitions to inactivated state but weaker transitions from low-to-high task demand states. Such dynamics of WM-related brain states appear to be constraited by structural connectivity. Our findings extend current understanding of how the FPN and DMN nodes are dynamically organized into a set of nuanced brain sates to support moment-to-moment information updating during WM and its links to structural connectivity. This line of research provides ample opportunities for future studies to further address on how the dynamical organization of large-scale functional brain networks, which is facilitated by structural connectivity and linked to structure–function coupling, contributes to cognitive development from childhood to adulthood.

Acknowledgments

We thank the National Center for Protein Sciences at Peking University in Beijing, China, for assistance with MRI data acquisition.

Authors' contributions

Ying He, Xinyuan Liang, Menglu Chen, Lei Hao, Jalil Taghia, and Shaozheng Qin performed formal analysis; Ying He, Yimeng Zeng, Ting Tian, Jiahua Xu, Rui Chen, Yanpei Wang, Jia-Hong Gao, Shuping Tan, Yong He, Sha Tao, Shaozheng Qin and Qi Dong performed and helped with investigation. Qi Dong, Sha Tao, Yong He and Shaozheng Qin performed conceptualization and supervision of the CBD project; Ying He, Xinyuan Liang, and Shaozheng Qin wrote the original draft; All authors commented and helped to write the review & editing.

Supplementary material

Supplementary material is available at *Cerebral Cortex* online.

Funding

This work is supported by the STI 2030—Major Projects 2021ZD0200500, the National Natural Science Foundation of China (32130045, 31522028, 82021004, and 31521063), the Beijing Brain Initiative of Beijing Municipal Science & Technology Commission (Z181100001518003), the Open Research Fund of the State Key Laboratory of Cognitive Neuroscience and Learning (CNLZD1503 and CNLZD1703), the Major Project of National Social Science Foundation (19ZDA363 and 20ZD153), and the Fundamental Research Funds for the Central Universities.
Conflict of interest statement: The authors declare no conflict of interests.

Ethical approval

All procedures performed in studies involving human participants were in accordance with the ethical standards of the institutional and/or national research committee and with the 1964 Helsinki declaration and its later amendments or comparable ethical standards.

Data availability

The data that support the findings of this study are available from the corresponding author upon reasonable request.

Code availability

Code used to generate the analyses are available at https://github.com/QinBrainLab/2022-BSDS-Working-memory.

References

Akshoomoff N. Selective attention and active engagement in young children. *Dev Neuropsychol*. 2002:22(3):625–642.
Alvarez JA, Emory E. Executive function and the frontal lobes: a meta-analytic review. *Neuropsychol Rev*. 2006:16(1):17–42.
Andersson JLR, Sotiropoulos SN. An integrated approach to correction for off-resonance effects and subject movement in diffusion MR imaging. *NeuroImage*. 2016:125:1063–1078.
Andersson JLR, Graham MS, Zsoldos E, Sotiropoulos SN. Incorporating outlier detection and replacement into a non-parametric framework for movement and distortion correction of diffusion MR images. *NeuroImage*. 2016:141:556–572.
Andersson JLR, Graham MS, Drobnjak I, Zhang H, Filippini N, Bastiani M. Towards a comprehensive framework for movement and distortion correction of diffusion MR images: within volume movement. *NeuroImage*. 2017:152:450–466.
Anticevic A, Cole MW, Murray JD, Corlett PR, Wang XJ, Krystal JH. The role of default network deactivation in cognition and disease. *Trends Cogn Sci*. 2012:16(12):584–592.
Avena-Koenigsberger A, Misic B, Sporns O. Communication dynamics in complex brain networks. *Nat Rev Neurosci*. 2018:19(1):17–33.
Basser PJ, Mattiello J, LeBihan D. MR diffusion tensor spectroscopy and imaging. *Biophys J*. 1994:66(1):259–267.
Bassett DS, Yang M, Wymbs NF, Grafton ST. Learning-induced autonomy of sensorimotor systems. *Nat Neurosci*. 2015:18(5):744–751.
Baum GL, Ciric R, Roalf DR, Betzel RF, Moore TM, Shinohara RT, Kahn AE, Vandekar SN, Rupert PE, Quarmley M, et al. Modular segregation of structural brain networks supports the development of executive function in youth. *Curr Biol*. 2017:27(11):1561–1572.e8.
Baum GL, Cui Z, Roalf DR, Ciric R, Betzel RF, Larsen B, Cieslak M, Cook PA, Xia CH, Moore TM, et al. Development of structure–function coupling in human brain networks during youth. *Proc Natl Acad Sci U S A*. 2020:117(1):771–778.
Bluhm RL, Clark CR, Mcfarlane AC, Moores KA, Shaw ME, Lanius RA. Default network connectivity during a working memory task. *Hum Brain Mapp*. 2011:32(7):1029–1035.

Bolton TAW, Morgenroth E, Preti MG, Van De Ville D. Tapping into multi-faceted human behavior and psychopathology using fMRI brain dynamics. *Trends Neurosci*. 2020:43(9):667–680.

Braun U, Schafer A, Walter H, Erk S, Romanczuk-Seiferth N, Haddad L, Schweiger JI, Grimm O, Heinz A, Tost H, et al. Dynamic reconfiguration of frontal brain networks during executive cognition in humans. *Proc Natl Acad Sci U S A*. 2015:112(37):11678–11683.

Braun U, Harneit A, Pergola G, Menara T, Schäfer A, Betzel RF, Zang Z, Schweiger JI, Zhang X, Schwarz K, et al. Brain network dynamics during working memory are modulated by dopamine and diminished in schizophrenia. *Nat Commun*. 2021:12(1):1–11.

Cai W, Warren SL, Duberg K, Pennington B, Hinshaw SP, Menon V. Latent brain state dynamics distinguish behavioral variability, impaired decision-making, and inattention. *Mol Psychiatry*. 2021: 26(9):4944–4957.

Casey BJ, Giedd JN, Thomas KM. Structural and functional brain development and its relation to cognitive development. *Biol Psychol*. 2000:54(1–3):241–257.

Chen M, He Y, Hao L, Xu J, Tian T, Peng S, Zhao G, Lu J, Zhao Y, Zhao H, et al. Default mode network scaffolds immature frontoparietal network in cognitive development. *Cereb Cortex*. 2022:1–13.

Cocchi L, Zalesky A, Fornito A, Mattingley JB. Dynamic cooperation and competition between brain systems during cognitive control. *Trends Cogn Sci*. 2013:17(10):493–501.

Cornblath EJ, Ashourvan A, Kim JZ, Betzel RF, Ciric R, Adebimpe A, Baum GL, He X, Ruparel K, Moore TM, et al. Temporal sequences of brain activity at rest are constrained by white matter structure and modulated by cognitive demands. *Commun Biol*. 2020:3(1): 1–12.

Crone EA, Bunge SA, Van Der Molen MW, Richard RK. Switching between tasks and responses: a developmental study. *Dev Sci*. 2006:9(3):278–287.

Cui Z, Stiso J, Baum GL, Kim JZ, Roalf DR, Betzel RF, Gu S, Lu Z, Xia CH, He X, et al. Optimization of energy state transition trajectory supports the development of executive function during youth. *elife*. 2020:9:1–60.

Curtis CE, D'Esposito M. Persistent activity in the prefrontal cortex during working memory. *Trends Cogn Sci*. 2003:7(9):415–423.

Damaraju E, Allen EA, Belger A, Ford JM, McEwen S, Mathalon DH, Mueller BA, Pearlson GD, Potkin SG, Preda A, et al. Dynamic functional connectivity analysis reveals transient states of dysconnectivity in schizophrenia. *NeuroImage Clin*. 2014:5:298–308.

Deco G, Jirsa VK, McIntosh AR. Emerging concepts for the dynamical organization of resting-state activity in the brain. *Nat Rev Neurosci*. 2011:12(1):43–56.

Deco G, Cruzat J, Cabral J, Tagliazucchi E, Laufs H, Logothetis NK, Kringelbach ML. Awakening: predicting external stimulation to force transitions between different brain states. *Proc Natl Acad Sci*. 2019:116(36):18088–18097.

Dosenbach NUF, Visscher KM, Palmer ED, Miezin FM, Wenger KK, Kang HC, Burgund ED, Grimes AL, Schlaggar BL, Petersen SE. A Core system for the implementation of task sets. *Neuron*. 2006:50(5):799–812.

Dosenbach NUF, Fair DA, Miezin FM, Cohen AL, Wenger KK, Dosenbach RAT, Fox MD, Snyder AZ, Vincent JL, Raichle ME, et al. Distinct brain networks for adaptive and stable task control in humans. *Proc Natl Acad Sci U S A*. 2007:104(26):11073–11078.

Dumontheil I, Klingberg T. Brain activity during a visuospatial working memory task predicts arithmetical performance 2 years later. *Cereb Cortex*. 2012:22(5):1078–1085.

Gergelyfi M, Jacob B, Olivier E, Zénon A. Dissociation between mental fatigue and motivational state during prolonged mental activity. *Front Behav Neurosci*. 2015:9:1–15.

Gu S, Pasqualetti F, Cieslak M, Telesford QK, Yu AB, Kahn AE, Medaglia JD, Vettel JM, Miller MB, Grafton ST, et al. Controllability of structural brain networks. *Nat Commun*. 2015:6(1): 8414.

Gu H, Schulz KP, Fan J, Yang Y. Temporal dynamics of functional brain states underlie cognitive performance. *Cereb Cortex*. 2021:31(4):2125–2138.

Hutchison RM, Morton JB. Tracking the brain's functional coupling dynamics over development. *J Neurosci*. 2015:35(17):6849–6859.

Hutchison RM, Morton JB. It's a matter of time: reframing the development of cognitive control as a modification of the brain's temporal dynamics. *Dev Cogn Neurosci*. 2016:18:70–77.

Hutchison RM, Womelsdorf T, Allen EA, Bandettini PA, Calhoun VD, Corbetta M, Della Penna S, Duyn JH, Glover GH, Gonzalez-Castillo J, et al. Dynamic functional connectivity: promise, issues, and interpretations. *NeuroImage*. 2013:80:360–378.

Ito J, Nikolaev AR, Van Leeuwen C. Dynamics of spontaneous transitions between global brain states. *Hum Brain Mapp*. 2007:28(9): 904–913.

Iuculano T, Moro R, Butterworth B. Updating working memory and arithmetical attainment in school. *Learn Individ Differ*. 2011:21(6): 655–661.

Jin C, Jia H, Lanka P, Rangaprakash D, Li L, Liu T, Hu X, Deshpande G. Dynamic brain connectivity is a better predictor of PTSD than static connectivity. *Hum Brain Mapp*. 2017:38(9):4479–4496.

Kellner E, Dhital B, Kiselev VG, Reisert M. Gibbs-ringing artifact removal based on local subvoxel-shifts. *Magn Reson Med*. 2016: 76(5):1574–1581.

Kottaram A, Johnston LA, Cocchi L, Ganella EP, Everall I, Pantelis C, Kotagiri R, Zalesky A. Brain network dynamics in schizophrenia: reduced dynamism of the default mode network. *Hum Brain Mapp*. 2019:40:2212–2228.

Kringelbach ML, Deco G. Brain states and transitions: insights from computational neuroscience. *Cell Rep*. 2020:32(10):108128.

Lebel C, Deoni S. The development of brain white matter microstructure. *NeuroImage*. 2018:182:207–218.

Lebel C, Gee M, Camicioli R, Wieler M, Martin W, Beaulieu C. Diffusion tensor imaging of white matter tract evolution over the lifespan. *NeuroImage*. 2012:60(1):340–352.

Lebel C, Treit S, Beaulieu C. A review of diffusion MRI of typical white matter development from early childhood to young adulthood. *NMR Biomed*. 2019:32(4):1–23.

Leung HC, Seelig D, Gore JC. The effect of memory load on cortical activity in the spatial working memory circuit. *Cogn Affect Behav Neurosci*. 2004:4(4):553–563.

Liang X, Sun L, Liao X, Lei T, Xia M, Duan D, Zeng Z, Xu Z, Men W, Wang Y. Structural connectome architecture shapes the maturation of cortical morphology from childhood to adolescence. *bioRxiv*. 2022.

Liegeois R, Li J, Kong R, Orban C, Van De Ville D, Ge T, Sabuncu MR, Yeo BTT. Resting brain dynamics at different timescales capture distinct aspects of human behavior. *Nat Commun*. 2019:10(1): 2317.

Ma L, Steinberg JL, Hasan KM, Narayana PA, Kramer LA, Moeller FG. Working memory load modulation of parieto-frontal connections: evidence from dynamic causal modeling. *Hum Brain Mapp*. 2012:33(8):1850–1867.

Marusak HA, Calhoun VD, Brown S, Crespo LM, Sala-Hamrick K, Gotlib IH, Thomason ME. Dynamic functional connectivity of neurocognitive networks in children. *Hum Brain Mapp*. 2017:38(1): 97–108.

Medaglia JD, Huang W, Karuza EA, Kelkar A, Thompson-Schill SL, Ribeiro A, Bassett DS. Functional alignment with anatomical

networks is associated with cognitive flexibility. *Nat Hum Behav*. 2018:2(2):156–164.

Medaglia JD, Satterthwaite TD, Kelkar A, Ciric R, Moore TM, Ruparel K, Gur RC, Gur RE, Bassett DS. Brain state expression and transitions are related to complex executive cognition in normative neurodevelopment. *NeuroImage*. 2018:166:293–306.

Owen AM, McMillan KM, Laird AR, Bullmore E. N-back working memory paradigm: a meta-analysis of normative functional neuroimaging studies. *Hum Brain Mapp*. 2005:25(1):46–59.

Pedersen M, Zalesky A, Omidvarnia A, Jackson GD. Multilayer network switching rate predicts brain performance. *Proc Natl Acad Sci U S A*. 2018:115(52):13376–13381.

Raichle ME, MacLeod AM, Snyder AZ, Powers WJ, Gusnard DA, Shulman GL. A default mode of brain function. *Proc Natl Acad Sci U S A*. 2001:98(2):676–682.

Ramirez-Mahaluf JP, Medel V, Tepper Á, Alliende LM, Sato JR, Ossandon T, Crossley NA. Transitions between human functional brain networks reveal complex, cost-efficient and behaviorally-relevant temporal paths. *NeuroImage*. 2020:219:117027.

Rashid B, Arbabshirani MR, Damaraju E, Cetin MS, Miller R, Pearlson GD, Calhoun VD. Classification of schizophrenia and bipolar patients using static and dynamic resting-state fMRI brain connectivity. *NeuroImage*. 2016:134:645–657.

Reddy PG, Mattar MG, Murphy AC, Wymbs NF, Grafton ST, Satterthwaite TD, Bassett DS. Brain state flexibility accompanies motor-skill acquisition. *NeuroImage*. 2018:171:135–147.

Reimers S, Maylor EA. Task switching across the life span: effects of age on general and specific switch costs. *Dev Psychol*. 2005:41(4):661–671.

Rubinstein JS, Meyer DE, Evans JE. Executive control of cognitive processes in task switching. *J Exp Psychol Hum Percept Perform*. 2001:27(4):763–797.

Ryali S, Supekar K, Chen T, Kochalka J, Cai W, Nicholas J, Padmanabhan A, Menon V. Temporal dynamics and developmental maturation of salience, default and central-executive network interactions revealed by variational Bayes hidden Markov modeling. *PLoS Comput Biol*. 2016:12(12):e1005138.

Seghier ML, Price CJ. Interpreting and utilising intersubject variability in brain function. *Trends Cogn Sci*. 2018:22(6):517–530.

Shine JM, Bissett PG, Bell PT, Koyejo O, Balsters JH, Gorgolewski KJ, Moodie CA, Poldrack RA. The dynamics of functional brain networks: integrated network states during cognitive task performance. *Neuron*. 2016:92(2):544–554.

Shine JM, Breakspear M, Bell PT, Ehgoetz Martens KA, Shine R, Koyejo O, Sporns O, Poldrack RA. Human cognition involves the dynamic integration of neural activity and neuromodulatory systems. *Nat Neurosci*. 2019:22(2):289–296.

Shu N, Liu Y, Li K, Duan Y, Wang J, Yu C, Dong H, Ye J, He Y. Diffusion tensor tractography reveals disrupted topological efficiency in white matter structural networks in multiple sclerosis. *Cereb Cortex*. 2011:21(11):2565–2577.

Sizemore AE, Bassett DS. Dynamic graph metrics: tutorial, toolbox, and tale. *NeuroImage*. 2018:180(Pt B):417–427.

Suárez LE, Markello RD, Betzel RF, Misic B. Linking structure and function in macroscale brain networks. *Trends Cogn Sci*. 2020:24(4):302–315.

Swendsen RH, Wang JS. Nonuniversal critical dynamics in Monte Carlo simulations. *Phys Rev Lett*. 1987:58(2):86–88.

Taghia J, Cai W, Ryali S, Kochalka J, Nicholas J, Chen T, Menon V. Uncovering hidden brain state dynamics that regulate performance and decision-making during cognition. *Nat Commun*. 2018:9(1):1–53.

Tang E, Giusti C, Baum GL, Gu S, Pollock E, Kahn AE, Roalf DR, Moore TM, Ruparel K, Gur RC, et al. Developmental increases in white matter network controllability support a growing diversity of brain dynamics. *Nat Commun*. 2017:8(1):1252.

Tomassy GS, Dershowitz LB, Arlotta P. Diversity matters: a revised guide to myelination. *Trends Cell Biol*. 2016:26(2):135–147.

Tomporowski PD, Davis CL, Lambourne K, Gregoski M, Tkacz J. Task switching in overweight children: effects of acute exercise and age. *J Sport Exerc Psychol*. 2008:30(5):497–511.

Tournier JD, Smith R, Raffelt D, Tabbara R, Dhollander T, Pietsch M, Christiaens D, Jeurissen B, Yeh CH, Connelly A. MRtrix3: a fast, flexible and open software framework for medical image processing and visualisation. *NeuroImage*. 2019:202:116137.

Tustison NJ, Avants BB, Cook PA, Zheng Y, Egan A, Yushkevich PA, Gee JC. N4ITK: improved N3 bias correction. *IEEE Trans Med Imaging*. 2010:29(6):1310–1320.

vander Meer JN, Breakspear M, Chang LJ, Sonkusare S, Cocchi L. Movie viewing elicits rich and reliable brain state dynamics. *Nat Commun*. 2020:11:1–14.

Vidaurre D, Quinn AJ, Baker AP, Dupret D, Tejero-Cantero A, Woolrich MW. Spectrally resolved fast transient brain states in electrophysiological data. *NeuroImage*. 2016:126:81–95.

Vidaurre D, Smith SM, Woolrich MW. Brain network dynamics are hierarchically organized in time. *Proc Natl Acad Sci U S A*. 2017:114(48):12827–12832.

Vidaurre D, Abeysuriya R, Becker R, Quinn AJ, Alfaro-Almagro F, Smith SM, Woolrich MW. Discovering dynamic brain networks from big data in rest and task. *NeuroImage*. 2018:180(Pt B):646–656.

Wang C, Hu Y, Weng J, Chen F, Liu H. Modular segregation of task-dependent brain networks contributes to the development of executive function in children. *NeuroImage*. 2019:116334:116334.

Wascher E, Rasch B, Sänger J, Hoffmann S, Schneider D, Rinkenauer G, Heuer H, Gutberlet I. Frontal theta activity reflects distinct aspects of mental fatigue. *Biol Psychol*. 2014:96:57–65.

Westin C-F. Geometrical diffusion measures for MRI from tensor basis analysis. Proc ISMRM'97. 1997.

Xiong B, Chen C, Tian Y, Zhang S, Liu C, Evans TM, Fernández G, Wu J, Qin S. Brain preparedness: the proactive role of the cortisol awakening response in hippocampal-prefrontal functional interactions. *Prog Neurobiol*. 2021:205:102127.

Yeh FC, Wedeen VJ, Tseng WYI. Generalized q-sampling imaging. *IEEE Trans Med Imaging*. 2010:29(9):1626–1635.

Yeo BT, Krienen FM, Eickhoff SB, Yaakub SN, Fox PT, Buckner RL, Asplund CL, Chee MWL. Functional specialization and flexibility in human association cortex. *Cereb Cortex*. 2015:25(10):3654–3672.

Yeung N, Monsell S. Switching between tasks of unequal familiarity: the role of stimulus-attribute and response-set selection. *J Exp Psychol Hum Percept Perform*. 2003:29(2):455–469.

Zalesky A, Fornito A, Harding IH, Cocchi L, Yücel M, Pantelis C, Bullmore ET. Whole-brain anatomical networks: does the choice of nodes matter? *NeuroImage*. 2010:50(3):970–983.

Zhuang L, Wang J, Xiong B, Bian C, Hao L, Bayley PJ, Qin S. Rapid neural reorganization during retrieval practice predicts subsequent long-term retention and false memory. *Nat Hum Behav*. 2022:6(1):134–145.